Research article

The Hsf1-sHsp cascade has pan-antiviral activity in mosquitoes

Jieqiong Qu, Michelle Schinkel, Lisa Chiggiato, Samara Rosendo Machado, Gijs J. Overheul, Pascal Miesen, Ronald P. van Rij *

Department of Medical Microbiology, Radboud Institute for Molecular Life Sciences, Radboud University Medical Center, P.O. Box 9101, 6500 HB Nijmegen, The Netherlands

* For correspondence: Ronald.vanRij@radboudumc.nl

Abstract

Aedes mosquitoes transmit pathogenic arthropod-borne (arbo) viruses, putting nearly half the world's population at risk. Blocking virus replication in mosquitoes is a promising approach to prevent arbovirus transmission, the development of which requires in-depth knowledge of virus-host interactions and mosquito immunity. By integrating multi-omics data, we find that heat shock factor 1 (Hsf1) regulates eight small heat shock protein (sHsp) genes within one topologically associated domain in the mosquito genome. This Hsf1-sHsp cascade acts as an early response against chikungunya virus (CHIKV) infection and shows pan-antiviral activity in three vector species, *Aedes aegypti*, *Aedes albopictus*, and *Anopheles gambiae* in cell experiments. Importantly, activation of Hsf1 leads to a reduced CHIKV infection rate in adult *Ae. aegypti* mosquitoes, establishing Hsf1 as a promising target for the development of novel intervention strategies to limit arbovirus transmission by mosquitoes.

Introduction

Aedes mosquitoes are the primary vectors of arthropod-borne (arbo) viruses [1] that pose significant health and economic burden to humans [2-4]. Dengue virus (DENV) alone causes approximately 400 million infections and 20,000 deaths annually [5]. Recent outbreaks of chikungunya virus (CHIKV) in Europe and the Americas have also garnered significant attention [6-11]. With the continued resurgence of arboviruses and their unprecedented geographical spread over the past years, there is a pressing need for novel strategies to prevent and mitigate future outbreaks.

Arbovirus transmission occurs primarily through a horizontal cycle between blood-feeding arthropod vectors, such as mosquitoes, and vertebrate hosts. Female mosquitoes ingest viruses during a blood meal from an infected host and then transfer viruses into a naïve host through biting [12, 13]. Blocking virus transmission at the mosquito stage, rather than solely targeting the virus in human hosts, constitutes a promising, alternative approach to prevent arbovirus spread [14]. The development of such approaches requires in-depth knowledge of mosquito antiviral immunity.

Our current understanding of the insect immune system is largely informed by studies in *Drosophila melanogaster* [15-18], where the RNA interference (RNAi) pathway serves as a major response that degrades viral RNA and inhibits replication [19-21]. Innate immune signaling pathways, specifically the NF-κB (Toll and IMD) and JAK-STAT pathways, have also been implicated in antiviral defense [16, 22]. However, *Drosophila* does not recapitulate mosquito specific processes such as virus acquisition and transmission via blood-feeding [12, 13, 15, 22]. It is therefore crucial to study immunity against arboviruses in relevant species, such as *Ae. aegypti*, the primary vector of the urban virus transmission cycle [23, 24].

RNAi has been identified as a major antiviral response in *Ae. aegypti* mosquitoes, with evidence from CHIKV [25], Zika virus (ZIKV) [26, 27], DENV [28, 29], and Sindbis virus (SINV) [30]. In contrast, the role of classical innate immune pathways is less well-defined and seems to be virus dependent [31-35]. For instance, ZIKV infection activates the Toll pathway, while DENV infection activates both the Toll and JAK-STAT pathways [31-33]. Activation of the Toll and JAK-STAT pathways by depleting pathway-specific negative regulators Cactus and PIAS, respectively, suppresses ZIKV infection [31]. On the other hand, activation of the IMD pathway by silencing of Caspar did not affect ZIKV infection [31], but impaired SINV replication [34]. Additionally, stimulation with either heat inactivated *E. coli* to activate

51 JAK-STAT and IMD pathways or *B. subtilis* to activate Toll pathway had no effect on CHIKV replication
52 [25], suggesting unknown antiviral mechanisms yet to be discovered.

53 To investigate the transcriptional responses of *Ae. aegypti* to viral infection, we conducted a time-
54 course RNA-seq experiment upon CHIKV infection. Our combined analyses of RNA-seq and chromatin
55 profiling data revealed an early-responsive cascade, consisting of heat shock factor 1 (Hsf1) driving the
56 expression of eight small heat shock proteins (sHsps). This Hsf1-sHsp cascade displayed conserved pan-
57 antiviral activities in *in vitro* experiments on three vector mosquitoes. Furthermore, activation of Hsf1
58 led to a reduced CHIKV infection rate *in vivo* in adult *Ae. aegypti* mosquitoes. As such, Hsf1 serves as
59 a promising target for the development of new intervention strategies to control arbovirus
60 transmission by mosquitoes.
61

62 ## Results

63 ### The Hsf1-sHsp cascade acts as an early response to CHIKV infection

64 To uncover novel components involved in antiviral defense in *Aedes* mosquitoes, we performed a
65 time-course RNA-seq experiment to determine differentially expressed genes (DEgenes) upon CHIKV
66 infection of *Ae. aegypti* Aag2 cells at 4, 8 and 48 hours post-infection (hpi) (Figure 1A and Table S1).
67 The CHIKV strain that emerged during the 2005–2006 outbreaks had acquired a mutation (A226V) in
68 the E1 envelope glycoprotein and was used in this study [36]. A multiplicity of infection (MOI) of 5 was
69 used to ensure that the vast majority of cells are synchronously infected and that DEgenes from
70 different time points represent transcriptional responses at different stages of infection. At 4 hpi, only
71 a single DEgene was detected (*AAEL000080*, encoding a putative phosphoenolpyruvate carboxykinase),
72 which was downregulated at 8 hpi. We observed major transcriptional changes at 8 hpi and 48 hpi,
73 which we termed the early and late responses to CHIKV infection, respectively. The late response was
74 more pronounced, with eight upregulated and 51 downregulated genes (Figure 1A), and KEGG
75 pathway analysis suggested that downregulated DEgenes were mainly involved in glycolysis, which we
76 have reported before [37]. In contrast, the early response was modest, with two downregulated and
77 19 upregulated genes, which were enriched for genes encoding HSP20-like chaperones (Figure 1A).
78 Protein domain analysis revealed four heat shock protein 70 (Hsp70) and eight small heat shock
79 proteins (sHsps) (Figure 1B), which function to prevent protein aggregation and to help cells to survive
80 stressful conditions [38].

While Hsp70 is involved in distinct steps of the viral cycle, including entry, RNA replication, and virion assembly [39, 40], the role of sHsps during virus infection is largely unknown [41]. Inspecting the genomic distribution of these sHsp genes, we found that all eight sHsps are encoded within one Topologically Associated Domain (TAD) deduced from Hi-C seq data [42] (Figure 1C), suggesting that these sHsp genes are likely to be coordinately regulated by the same cis-regulatory network [43, 44]. To further study the regulation of sHsp gene expression within this TAD, we mapped our chromatin profiling data from Aag2 cells [45], and performed motif scan within open chromatin regions defined by the Assay for Transposase-Accessible Chromatin with sequencing (ATAC-seq). We found the DNA binding motif of the transcription factor heat shock factor 1 (Hsf1) to be highly enriched at promoter regions of these eight sHsp genes, but not at other genes within the same TAD (Figure 1D). These regions were also marked by active histone marks H3K4me3 and H3K27ac, as well as RNA polymerase II occupancy, indicating active transcription [46, 47]. These findings together suggest that Hsf1 is the transcription factor that regulates sHsp gene expression. To experimentally test this hypothesis, we RNAi silenced *Hsf1*, and indeed, the induction of all eight *sHsps* upon CHIKV infection was significantly diminished (Figure 1E). Hence, the Hsf1-sHsp cascade functions as an early transcriptional response to CHIKV infection in Aag2 cells.

The Hsf1-sHsp cascade displays a broad antiviral activity

To explore the antiviral potential of the identified Hsf1-sHsp axis, we silenced *Hsf1* using RNAi and observed elevated CHIKV RNA levels (Figure 2A). sHsp genes share high similarity at the nucleotide level, we therefore used two sets of dsRNA targeting the conserved Hsp20 domain to knock down all 8 sHsp genes and observed significantly increased CHIKV RNA copies (Figure 2B). In parallel, we knocked down *Hsp70*, which did not affect CHIKV replication (Figure 2C). These results together suggested that the Hsf1-sHsp axis has antiviral activity against CHIKV infection.

We then modulated the activity of Hsf1 with either the small molecule inhibitor KRIBB11 [48], or the activator hsfa1 [49]. KRIBB11 inhibits Hsf1-dependent recruitment of positive Transcription Elongation Factor b to the promoters of target genes, thus blocking gene activation [48]. Indeed, KRIBB11 treatment did not affect *Hsf1* expression, but led to more than 5-fold increase of viral RNA levels in Aag2 cells at 12 hpi of CHIKV infection (Figure 2D). The effect of KRIBB11 on virus replication remained concordant at 24 hpi. While the expression of most *sHsps* was significantly reduced with KRIBB11 treatment, counterintuitively, we observed de-repression or even activation of some *sHsps*, such as

111 *AAEL013346*, *AAEL013349*, and *AAEL013351* at 12 hpi, which is likely a secondary effect resulting from
112 the increased CHIKV replication (Figure 2D). The precise mechanism by which hsfa1 activates Hsf1 is
113 not yet understood [49]. We observed a significant increase in the *Hsf1* expression upon hsfa1
114 treatment, and accordingly a strong activation of all eight *sHsp* genes. Importantly, hsfa1 treatment
115 led to about 25-fold reduction in CHIKV copies at 12 hpi and about 10-fold reduction at 24 hpi (Figure
116 2D), which is in agreement with our RNAi experiments and thus substantiates the antiviral role of sHsps.

117 Next, we tested the effect of these compounds on replication of other alphaviruses, including SINV
118 (AR339 strain, Figure 2E), the insect-specific Agua Salud alphavirus (ASALV, Figure 2F), and the
119 flavivirus DENV (serotype 2, Figure 2G). Consistently, KRIBB11 treatment led to increased virus
120 replication, whereas hsfa1 treatment significantly reduced virus replication (Figures 2E-G). We then
121 extended our findings to *in vitro* experiments of other mosquito species and confirmed the antiviral
122 property of the Hsf1-sHsp cascade in several natural virus-vector combinations [50, 51], such as CHIKV
123 in *Aedes albopictus* U4.4 cells (Figure 2H) and C6/36 cells (Figure 2I), and O'nyong-nyong (ONNV) in
124 *Anopheles gambiae* Mos55 cells (Figure 2J). The fact that the heat shock response was antiviral in both
125 U4.4 cells and the RNAi-deficient C6/36 cells indicates that the Hsf1-sHsps cascade functions
126 independently of RNAi. Together, these results suggest that the newly defined Hsf1-sHsp pathway
127 displays a pan-antiviral role in cells from all three tested mosquito species.

128 To identify which stage of the virus life cycle is affected by the Hsf1-sHsp cascade, we performed time-
129 of-addition assays in Aag2 cells treated with either hsfa1 or KRIBB11 at different time points relative
130 to inoculation with CHIKV (Figure 3A and Figure S1A). When hsf1a was added at time points before
131 inoculation up to 4 hpi, CHIKV replication was strongly inhibited (Figure 3B), indicating that hsfa1 does
132 not affect the virus attachment or entry step. After 4 hpi, both positive and negative sense viral RNA
133 copies reached a detectable level and the inhibitory effect of hsf1a on CHIKV replication started to
134 diminish gradually (Figure 3B), suggesting that the Hsf1-sHsp cascade interacts with the early stage of
135 virus RNA replication. In agreement, time-of-addition assay with KRIBB11 treatment showed the same
136 pattern (Figure S1).

137 To sum up, we demonstrated that the Hsf1-sHsp cascade displays a broad antiviral activity in mosquito
138 cells, likely via reducing early virus replication. As such, the upstream transcription factor, Hsf1, serves
139 as a potential target for developing antiviral interventions in mosquitoes.

140 ***In vivo* antiviral activity of the Hsf1-sHsp cascade**

141 We next sought to determine the antiviral activity of the identified Hsf1-sHsp cascade in mosquitoes.
142 Using RNA-seq, we first evaluated the baseline expression of *sHsp* genes, which varied dramatically
143 across different tissues of female *Ae. aegypti* (Figure 4A). Interestingly, *sHsp* genes were expressed at
144 low levels in two main barrier tissues, the midgut and salivary glands, compared to other tissues such
145 as the crop (Figure 4A).

146 To assess whether the Hsf1-sHsp cascade is activated as a natural antiviral response against CHIKV
147 infection, we first established the *in vivo* CHIKV infection kinetics in *Ae. aegypti* mosquitoes (Figure
148 S2A) and subsequently examined different tissues at 3 d and 5 d post blood feeding (dpf) when the
149 virus had disseminated to most body parts (Figures S2B and S2C). Midguts and salivary glands showed
150 comparable CHIKV RNA levels at 3 dpf, while salivary glands showed the highest CHIKV RNA levels at
151 5 dpf (Figure S2B). Despite relatively uniform CHIKV RNA levels, *sHsp* expression fluctuated within each
152 tissue. Interestingly, a minor induction of some *sHsp* genes (*e.g.*, *AAEL013344*) was observed in ovaries,
153 but not in other tissues (Figure S2C), suggesting that specific sHsps may play a protective role in ovaries
154 against CHIKV infection.

155 We then explored the possibility of activating Hsf1 in mosquitoes with small molecule compounds.
156 Due to the poor solubility of hsfa1 and KRIBB11 in blood, we could not continue with these two
157 compounds in *in vivo* experiments. Instead, we tested another compound, Direct Targeted Hsf1
158 InhiBitor (DTHIB), which has been reported as a direct human Hsf1 inhibitor by stimulating the
159 degradation of nuclear Hsf1 [52]. Unexpectedly, DTHIB treatment did not affect *Hsf1* expression but
160 resulted in a dose-dependent activation of *sHsp* expression in Aag2 cells (Figures 4B-C). Thus, rather
161 than an inhibitor, DTHIB acts as an Hsf1 activator in mosquito cells. Indeed, in line with our
162 observations with hsf1a, treatment with DTHIB strongly reduced CHIKV replication in Aag2 cells (Figure
163 4B).

164 Next, we administered DTHIB to 3–5-day-old female *Ae. aegypti* mosquitoes via blood meal in the
165 absence of CHIKV, with DMSO serving as a control. At 3 dpf, midguts and carcasses were dissected to
166 check the stimulation of sHsps when the blood meal has been completely digested. We observed a
167 significantly increased expression of AAEL013350 in carcasses but not in midgut (Figure S3). It is
168 possible that the induction of sHsps in midguts are earlier than 3 dpf, however, it is technically difficult
169 to evaluate the expression level of sHsps at earlier time points due to the large amount of blood meal
170 retained in the midgut. In parallel, we administered DTHIB to 3–5-day-old female *Ae. aegypti*

171 mosquitoes via blood meal in the presence of CHIKV. We assessed the infectious titers at 3 dpf and did
172 not observe a significant difference (Mann-Whitney test, Figure 4D), however, there was a significant
173 reduction in the infection rate, from 62% to 33%, with DTHIB treatment (Figure 4D), indicating that
174 activation of Hsf1 presents a bottleneck to CHIKV infection in *Ae. aegypti* mosquitoes.

175 **Discussion**

176 Our combined analyses of RNA-seq and epigenetic profiling data revealed an early-responsive Hsf1-
177 sHsp cascade activated upon CHIKV infection, which we found to have broad *in vitro* antiviral activity
178 against alphaviruses and a flavivirus in three vector mosquito species: *Ae. aegypti*, *Ae. albopictus*, and
179 *An. gambiae*. *In vivo* activation of Hsf1 resulted in a significant decrease in the CHIKV infection rate in
180 *Ae. aegypti* mosquitoes. Overall, our work uncovers a novel antiviral cascade Hsf1-sHsp and identifies
181 Hsf1 as a potential target for developing transmission-blocking strategies against arboviruses (Figure
182 4E).

183 While RNAi is a well-established antiviral mechanism in mosquito vectors, it is becoming evident that
184 inducible signaling pathways are of vital importance as well. In addition to the classical Toll, IMD, and
185 JAK-STAT pathways, Wnt, mTOR, Ras/ERK, c-jun pathways, and the Hsf1-sHsp cascade identified in this
186 study, have been implicated in antiviral host defense [31, 33, 34, 53-55]. The temporal activation of
187 signaling pathways and associated genes is precisely regulated, as revealed by our time-course RNA-
188 seq data. The activation of *sHsp* genes is mainly restricted to the early stage and is not detectable in
189 the late stage of CHIKV infection. In line with our findings, published RNA-seq data from an *in vivo*
190 study of *Ae. aegypti* mosquitoes showed a similar pattern, with a higher induction of *sHsp* expression
191 at the early stage (3 dpi) than at the late stage (7 dpi) of CHIKV infection [41]. To gain deeper insights
192 into the regulation of *sHsp* genes, we performed integrative analyses of 3D chromatin conformation
193 (Hi-C seq) and chromatin profiling data (ATAC-seq and ChIP-seq), and identified Hsf1 as the upstream
194 transcription factor that regulates expression of eight *sHsp* genes within one TAD. Targeting the
195 transcription factor Hsf1, rather than individual downstream genes, is expected to be more effective
196 for antiviral control. Indeed, when we activated Hsf1 in adult mosquitoes, we observed a significant
197 decrease in the CHIKV infection rate. Together, our multi-omics analysis strategy demonstrates its
198 power in discovering novel antiviral signaling pathways, which can be applied to further investigate
199 virus-vector interactions in different tissues, in other mosquito species, and in other arbovirus
200 infections.

201 While Hsp70 is required at various stages of the viral cycle including entry, RNA replication, and virion
202 assembly [39, 40, 56, 57], few studies analyzed the role of sHsps in viral infection [41]. This may be due
203 to their transient activation pattern during the early stages of virus infection; this dependency on virus
204 infection dynamics may make sHsp activation difficult to be captured. As arboviruses need to
205 overcome tissue barriers to establish a persistent infection of the mosquito, the infection state of
206 different tissues or body parts are highly variable. This could potentially explain why we failed to
207 observe robust *sHsp* induction upon CHIKV blood feeding in different tissues. Yet, *AAEL013344*, one of
208 the *sHsp* genes, was found to be upregulated upon ZIKV infection [57]. Further investigation is needed
209 to assess whether *sHsp* genes are coordinately upregulated by specific arboviruses, and single-cell
210 RNA-seq may be a useful tool to address the heterogeneity of sHsp activation.

211 The mechanism underlying the antiviral activity of the Hsf1-sHsp cascade remains largely elusive. Our
212 time-of-addition assays suggest that the response inhibits an early post-entry stage of the viral
213 replication cycle. As Hsf1 activation led to a broad antiviral effect in three vector mosquitoes, it is likely
214 that the Hsf1-sHsp cascade interacts, either directly or indirectly, with a common viral protein feature
215 or a conserved host protein complex. It has been suggested that sHsps maintain protein homeostasis
216 by binding proteins in non-native conformations, thereby preventing substrate aggregation [58]. The
217 fact that a wide range of proteins is protected from precipitation suggests that sHsps may act rather
218 promiscuously, similarly to the molecular chaperone Hsp70 [58-62]. It will be of great interest to profile
219 sHsp associated proteins using proteomic approaches to identify sHsp client proteins and shed light
220 on its antiviral mechanism.

221 To sum up, we identified the Hsf1-sHsp cascade as a novel antiviral mechanism in mosquitoes and
222 propose Hsf1 as a potential target for developing arbovirus-blocking interventions. Considering the
223 pan-antiviral activity of the Hsf1-sHsp cascade, our findings may open the way for the development of
224 a broad-spectrum drug to prevent arbovirus transmission.

225 ## Materials and Methods

226 ### Cell lines

227 *Ae. aegypti* Aag2 cells were kindly provided by Raul Andino (University of California San Francisco), *Ae.*
228 *albopictus* U4.4 cells were kindly provided by Gorben Pijlman (Wageningen University), and C6/36 cells
229 were obtained from ECACC General Cell Collection (#89051705). All these three cell lines were grown
230 in Leibovitz's L-15 medium (Gibco 21083-027) supplemented with 10% fetal bovine serum (Sigma
231 F7524-500ML), 50 U/ml Penicillin, 50 µg/mL Streptomycin (Gibco 15070-063), 1x non-essential Amino
232 Acids (Gibco 11140-035) and 2% Tryptose phosphate broth solution (Sigma T8159-100ML). *An.*
233 *gambiae* Mos55 cells were kindly provided by Jason L. Rasgon (The Pennsylvania State University) and
234 were grown in Schneider's insect medium (Gibco 21720024) supplemented with 10% fetal bovine
235 serum, 50 U/ml Penicillin, and 50 µg/mL Streptomycin. These cell lines were cultured at 28°C without
236 CO_2. BHK-15 and BHK-21 cells were grown in Dulbecco's modified Eagle medium (Gibco 41965039),
237 supplemented with 10% fetal bovine serum, 50 U/mL penicillin, and 50 µg/mL streptomycin. These
238 mammalian cells were cultured at 37°C, with 5% CO_2.

239 ### Viruses

240 The CHIKV expression plasmid encoding the Leiden synthetic (LS3, GenBank: JX911334.1) wildtype
241 strain was kindly provided by Dr. M.J. van Hemert (Leiden University Medical Center) and viral RNA
242 was obtained by *in vitro* transcription on linearized plasmids using T7 mMessage mMachine (Invitrogen
243 AM1344) [36]. RNA was then transfected into BHK-21 to grow the infectious virus. SINV AR339 strain
244 (pTE3' 2J) was obtained by transfecting *in vitro* transcribed RNA from pTE3' 2J in BHK-21 cells [63].
245 ASALV (GenBank: MK959114), kindly provided by Sandra Junglen (Charité, Berlin), was originally
246 isolated from the homogenate of mosquito pool MP416 and grown in C6/36 cells [64]. ONNV plasmid
247 was kindly provided by Prof. Dr. Andres Merits (University of Tartu), *in vitro* transcribed and grown in
248 C6/36 cells [65]. DENV serotype 2 (DENV2, strain 16681) was provided by Beate Kümmerer (University
249 of Bonn) and stocks were prepared on C6/36 cells. For the quantification of viral stocks, CHIKV, SINV,
250 and ONNV were titrated by end-point dilution on BHK-21 cells, DENV2 was titrated on BHK-15 cells,
251 and ASALV was titrated on C6/36 cells. A day before the titration, $1x10^4$ mammalian or $5x10^4$ C6/36
252 cells were seeded per well in a 96-well flat bottom plate. A 10-fold serial dilution of virus samples was
253 added to the cells in quadruplicate for the titration. After an incubation time of 5 days, cells were

254 inspected for cytopathic effect. The virus titer was calculated according to the Reed and Muench
255 method [66].

256 **Mosquito experiment**

257 *Ae. aegypti* mosquitoes (Black Eye Liverpool strain) were obtained from BEI Resources and were reared
258 at 28 °C, with 70% humidity and automated room lighting set at a 12:12 hours light/dark cycle. Larvae
259 were fed with Tetramin Baby fish food (Tetra). Adult mosquitoes were fed with a 10% sucrose solution.
260 Three-to-five-day-old female mosquitoes were used for experiments unless stated otherwise.

261 For blood feeding experiments, mosquitoes were starved for 24 h prior to the experiment. CHIKV virus
262 stock (5×10^8 $TCID_{50}$/mL) and full human blood (Sanquin) was 1:2 mixed to make the infectious blood
263 meal with a final virus titer of 1.7×10^8 $TCID_{50}$/ml. DMEM medium was mixed in the same ratio with
264 human blood to prepare the mock inoculum. Blood feeding was performed with the Hemotek system
265 for half an hour. Afterwards, mosquitoes were anesthetized on a CO_2 pad. Only blood fed mosquitoes
266 were selected and kept in culture until the indicated time points. Mosquitoes were tissue dissected as
267 previously described [67]. Whole mosquitoes, dissected body parts or tissues were homogenized in
268 either 200 µl DMEM medium for end-point titration on BHK-21 cells or in 1 mL RNA-Solv reagent
269 (Omega Bio-Tek) for RNA isolation, using a Precellys 24 homogenizer program 5 (Bertin technologies).

270 **RNAi in mosquito cells**

271 PCR products flanked by T7 promoter sequences at both ends were *in vitro* transcribed by T7
272 polymerase to produce dsRNA. These PCR products were *in vitro* transcribed using a homemade T7
273 RNA polymerase. For the formation of double-stranded RNA, the reactions were heated to 90 °C for
274 10 minutes and then allowed to gradually cool to room temperature and RNA was purified using the
275 GenElute Mammalian Total RNA kit (Sigma RTN350) according to the manufacturer's protocol. Two
276 sets of dsRNA targeting the Hsp20 domain were used to knock down *sHsp* expression (Figure 2B) and
277 two sets of dsRNA targeting the Hsp70 domain were used to knock down *Hsp70* (Figure 2C). For
278 detailed oligonucleotide information, see Table S2.

279 Aag2 cells were seeded at a density of $1.5\text{x}10^5$ cells/well in a 24-well plate, 24 h before the dsRNA
280 transfection. For each target gene, a transfection mix containing 300 µl non-supplemented L-15
281 medium, 500 ng dsRNA, and 1.3 µl X-treme GENE HP DNA transfection reagent (Roche 6366546001)

282 was prepared according to the manufacturer's recommendations. Per well, 100 µl of the transfection
283 mix was added in a dropwise manner. Cell culture medium was refreshed at 4 h post-transfection.
284 Three days post-transfection, cells were either harvested for evaluation of target gene knockdown or
285 infected with CHIKV at a MOI of 5.

286 **RNA isolation and RT-qPCR**

287 Aag2 cells were homogenized in RNA-Solv reagent (Omega Bio-Tek) and RNA extraction was
288 performed according to the manufacturer's instructions. Briefly, 200 µl of chloroform was added to 1
289 mL RNA-Solv reagent, and thoroughly mixed. After centrifugation, the aqueous phase was collected,
290 and RNA was precipitated using isopropanol. This mix was incubated for 1 hour at 4 °C followed by
291 centrifugation to pellet the RNA. Pellets were washed twice in 80% ethanol, and dissolved in nuclease
292 free water. RNA integrity was evaluated on ethidium bromide-stained agarose gels, and RNA
293 concentration was determined using the Nanodrop ND-1000.

294 For RT-qPCR analyses, DNaseI (Ambion)-treated RNA was reverse transcribed with random hexamers
295 using the TaqMan Reverse Transcription Reagents (Invitrogen N8080234) and PCR amplified using the
296 GoTaq qPCR system (Promega A6002) on a LightCycler 480 (Roche). In RNAi experiments, expression
297 levels of target genes were normalized to the expression of the housekeeping gene *lysosomal aspartic*
298 *protease* (*LAP*, *AAEL006169*), and fold changes were calculated using the 2-ΔΔCT method [68]. All
299 primers are listed in Table S2.

300 **RNA-seq library preparation and analysis**

301 For RNA sequencing in Aag2 cells, control dsRNA (dsLuc) treated cells were infected with CHIKV at a
302 MOI of 5. The double stranded RNA treatment was included in the procedure to allow a better
303 comparison of the 4 hpi and 8 hpi samples to the 48 hpi datasets that was generated in parallel for a
304 previously published study (PRJNA885496) [37].

305 Three-to-five-day-old female mosquitoes were anesthetized on a CO_2 pad, washed once in 70%
306 ethanol and three times with 1× PBS for outer de-contamination. Afterwards, crop, fat body, leg,
307 Malpighian tubules, midgut, ovary, salivary glands, and wings were dissected. Tissues from about 20
308 mosquitoes were pooled to achieve enough RNA (1 µg) for RNA-seq library preparation. Three batches
309 of mosquitoes were dissected and the corresponding RNA samples serve as biological triplicates for

310 RNA-seq. TruSeq Stranded mRNA kit (Illumina 20020594) was used for library preparation from total
311 RNA according to the manufacturer's protocol. The prepared libraries were quantified and controlled
312 for sample quality using High Sensitivity DNA Chip on a DNA1000 Bioanalyzer (Agilent 5067-4626), and
313 the libraries were analyzed on an Illumina HiSeq 4000 sequencer (GenomEast Platform). RNA-seq is
314 deposited in GEO database (GSE225070).

315 After initial quality control by FastQC [69], raw sequence reads were aligned to the reference genome,
316 *Ae. aegypti* LVP (Vectorbase, release 56), using STAR [70] with default settings. Quantification of gene
317 expression (FPKM) was performed with Cuffdiff [71]. R package DESeq2 was used for differential gene
318 expression analysis (with adjusted p value < 0.05) [72]. Genes were considered expressed if the mean
319 of the DESeq2-normalized counts (basement) was higher than 20. The R package pheatmap was used
320 to generate the heatmap for DEgenes upon CHIKV infection, which was based on z-scores of
321 normalized gene expressions ($\log_{10}$ FPKM) [73]. DEgenes are listed in Table S1.

322 **Bioinformatic analyses**

323 STRING was used for KEGG pathway and InterPro protein domain enrichment analysis [74]. Detailed
324 protein domain analysis was performed using InterPro [75].

325 For 3D chromatin conformation analysis, TADs were defined by analyzing Hi-C data (GSE95797) [42]
326 with HiCExplorer [76]. A cut off of p < 0.05 was used, after correcting for multiple tests.
327 pyGenomeTracks from the deepTools package [77] was used to visualize gene expression pattern,
328 TADs, and previously published chromatin profiling data from Aag2 cells, including ATAC-seq, histone
329 mark ChIP-seq and RNA pol II ChIP-seq (GSE210270) [45]. All genome browser tracks were normalized
330 to FPKM (y-axis). Open chromatin regions were defined as ATAC-seq peaks called by MACS2 with
331 standard settings and a q value of 0.05 [78]. Homer was used for DNA motif scan on ATAC-seq peaks
332 [79].

333 **Compound experiment**

334 KRIBB11 (2538), Hsf1a (1890), and DTHIB (3412) were purchased from Axon Medchem. All compounds
335 were dissolved in DMSO to final concentrations of 10 mM (KRIBB11) or 100 mM (Hsf1a and DTHIB)
336 and stored at 4°C for use within one month. Mosquito cells were seeded at a density of 1.5×10^5
337 cells/well in a 24-well plate. When cells reach 50% confluency, cells were treated with the indicated

338 concentrations of compound or an equivalent volume of DMSO and immediately afterwards
339 inoculated with virus at the indicated MOI. Cell lysates were collected at indicated time points post-
340 infection for RT-qPCR. For the time-of-addition assay, the same procedures were followed, except that
341 the medium was replaced at 1 hpi. For mosquito experiments, compound was directly added to
342 infectious blood meal and mixed well before blood feeding, with DMSO serving as a control.

343 **Quantification and statistical analysis**

344 RT-qPCR experiments in Figures 1E, 2, and S3 were performed in biological triplicate, quintuplicate,
345 sextuplicate, or octuplicate, with individual data shown as dot and the bars indicating mean ± SD.
346 Statistical differences were examined by unpaired t-test. For RT-qPCR in Figure 4B, one-way ANOVA
347 was performed. For virus titer comparison in Figure 4D, nonparametric Mann-Whitney U test was
348 performed. For the infection rate comparison in Figure 4D, Chi-squared test was performed. All
349 statistical significance in this study were produced by GraphPad Prism 9.

350 **Resource availability**

351 **Lead contact**

352 Further information and requests for resources and reagents should be directed to and will be fulfilled
353 by the lead contact, Ronald P. van Rij (Ronald.vanRij@radboudumc.nl).

354 **Materials availability**

355 Sequences of DNA oligo are available in Table S2. This study did not generate new unique reagents.

356 **Data availability**

357 Newly generated sequencing data have been deposited at GEO (GSE225070) and will be publicly
358 available at the date of publication. This paper analyzes existing, publicly available data. The accession
359 numbers for the datasets are listed in the Key Resources Table. This paper does not report original
360 code. Any additional information required to reanalyze the data reported in this paper is available
361 from the lead contact upon request.

362

Acknowledgments

We thank Martijn van Hemert (Leiden University Medical Center), Sandra Junglen (Charité Universitätsmedizin Berlin), Andres Merits (University of Tartu), Beate Kümmerer (University of Bonn), and Jason Rasgon (Pennsylvania State University) for providing materials. We thank BEI resources established by the National Institute of Allergy and Infectious Diseases for providing *Aedes aegypti* Liverpool mosquitoes. We thank Benoit Besson, Finny Varghese, and other members of the laboratory for fruitful discussions. This work is supported by a VENI grant from the Dutch Research Council to P.M. (grant number VI.Veni.202.035) and a VICI grant from the Dutch Research Council to R.P.v.R. (grant number 016.VICI.170.090).

Author Contributions

J.Q., P.M., and R.P.v.R designed the experiments and analyzed the data. J.Q. performed computational analyses. J.Q., M.S., L.C., S.R.M., and G.O., performed the experiments. J.Q. and R.P.v.R. wrote the paper. All authors read and contributed to the manuscript.

Competing Interest Statement

The authors declare no competing interests.

Figures

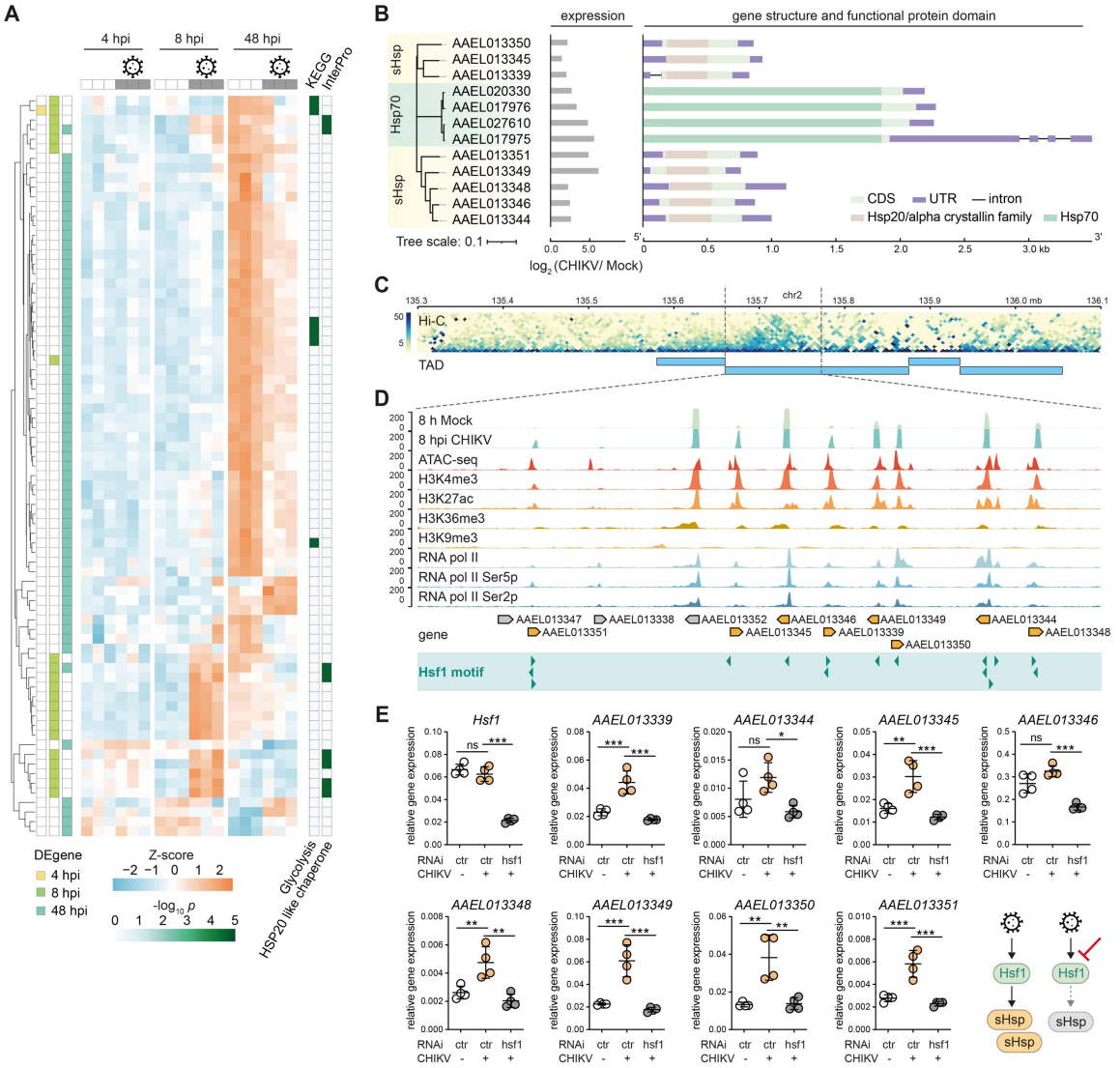

Figure 1. Hsf1 activates sHsps during the early stage of CHIKV infection.

(A) Hierarchical clustering of differentially expressed (DE) genes at 4, 8, and 48 hpi of CHIKV infection (MOI = 5), as quantified from RNA-seq data. DEgenes ($p < 0.05$) at each time point are color labeled on the left; KEGG pathway and InterPro enrichment is shown on the right. Z scores were calculated based on log-transformed Fragments per Kilobase per Million mapped reads (FPKM).

(B) Gene structure and protein domain analysis of heat shock proteins upregulated at 8 hpi of CHIKV infection. A neighbor-joining tree was constructed based on amino acid sequences (left). The $\log_2$ fold change in gene expression was quantified by RNA-seq (middle). The gene structure and InterPro protein domains are shown along the gene body (right).

(C) Hi-C interaction track with topologically associated domains (TADs) shown as horizontal blue bars ($p < 0.05$).

393 (D) Genome browser tracks showing RNA-seq data of mock and CHIKV infected Aag2 cells and
394 chromatin profiling data from uninfected Aag2 cells (ATAC-seq, histone marks and RNA pol II ChIP-seq)
395 within the indicated TAD. Eight upregulated *sHsp* genes at 8 hpi are highlighted in orange, other genes
396 in gray. Predicted Hsf1 motifs are shown as green arrowheads at the bottom.
397 (E) Expression of the indicated genes in CHIKV (MOI = 5) (+) or mock (-) infected Aag2 cells upon RNAi-
398 mediated silencing of *Hsf1* at 8 hpi. Luciferase dsRNA served as a non-targeting control (ctr). RT-qPCR
399 was performed in biological quintuplicates and shown as dots, with horizontal lines and the bars
400 indicating mean ± SD. Symbols denote statistical significance in unpaired t-tests (ns, not significant, * p
401 < 0.05, ** $p < 0.01$, *** $p < 0.001$).

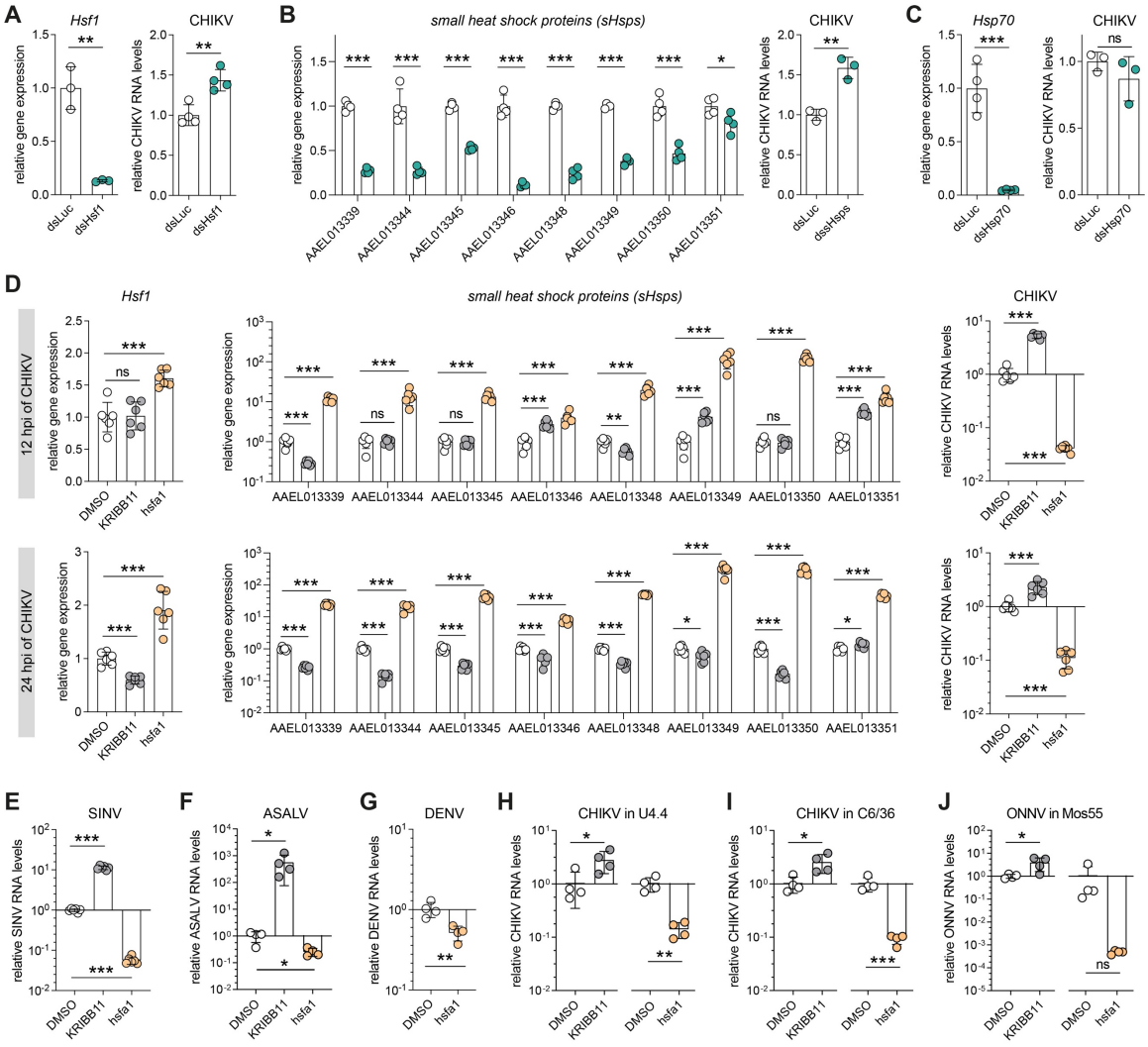

Figure 2. Pan-antiviral activity of the Hsf1-sHsp axis

(A-C) RNAi silencing of *Hsf1* (A), *sHsps* (B), *Hsp70* (*AAEL017975*) (C), and quantification of CHIKV RNA copies. RT-qPCR was used to assess target gene knockdown in uninfected Aag2 cells (left) and to quantify CHIKV mRNA copies at 8 hpi (MOI = 5) after target gene knockdown (right) in biological triplicate or quadruplicate, with luciferase dsRNA (dsLuc) serving as a non-targeting control. Original data are shown as dots, with bars indicating mean ± SD. Symbols denote statistical significance in unpaired t-tests (ns, not significant, * $p < 0.05$, ** $p < 0.01$, *** $p < 0.001$).

(D) Treatment with either Hsf1 inhibitor KRIBB11 (10 µM) or Hsf1 activator hsfa1 (100 µM). RT-qPCR was performed to analyze the expression of *Hsf1* (left), *sHsps* (middle), and changes in CHIKV RNA copies (right) at 12 and 24 hpi of CHIKV (MOI = 5), with DMSO serving as a control.

(E-G) Viral RNA levels in Aag2 cells treated with KRIBB11 (10 µM) or hsfa1 (100 µM) at 12 hpi of Sindbis virus (SINV, MOI = 5) (E), at 12 hpi of Agua Salud alphavirus (ASALV, MOI = 5) (F), and at 72 hpi of dengue virus (DENV, MOI = 0.01) (G).

(H-J) Viral RNA levels upon treatment with KRIBB11 (5 µM) and hsfa1 (100 µM) at 12 hpi of CHIKV (MOI = 5) in U4.4 cells (H), at 12 hpi of CHIKV (MOI = 5) in C6/36 cells (I), at 48 hpi of o'nyong'nyong virus

419 (ONNV, MOI = 0.5) in Mos55 cells (J). RT-qPCR was performed in biological quadruplicate or
420 sextuplicate, shown as dots, with the bars indicating mean ± SD. Symbols denote statistical significance
421 in unpaired t-tests (ns, not significant, * $p < 0.05$, ** $p < 0.01$, *** $p < 0.001$).

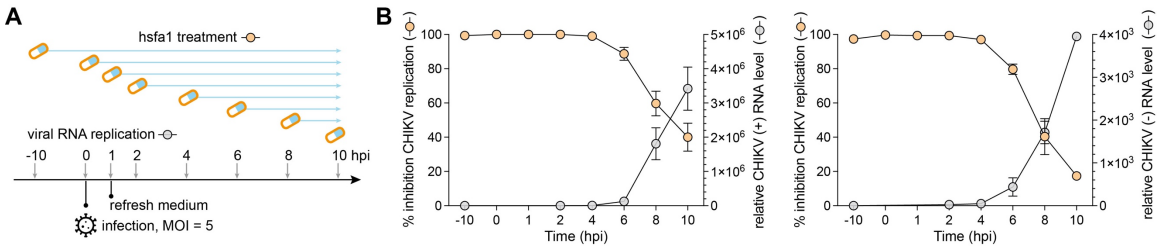

Figure 3. hsfa1 inhibits the early stage of CHIKV replication.

(A) Schematic illustration of the time-of-addition assay, with hsfa1 added at different time points during CHIKV infection (MOI = 5). Cell culture medium was refreshed to wash away unbound virus particles at 1 hpi. Cells treated with either hsfa1 (orange) or DMSO (gray) were harvested at each indicated time point.

(B) The effect of hsfa1 (100 μM) on virus replication was determined with RT-qPCR on both positive sense RNA (+, left) and negative sense RNA (-, right). Data are presented as means ± SD of three independent experiments, with DMSO serving as control.

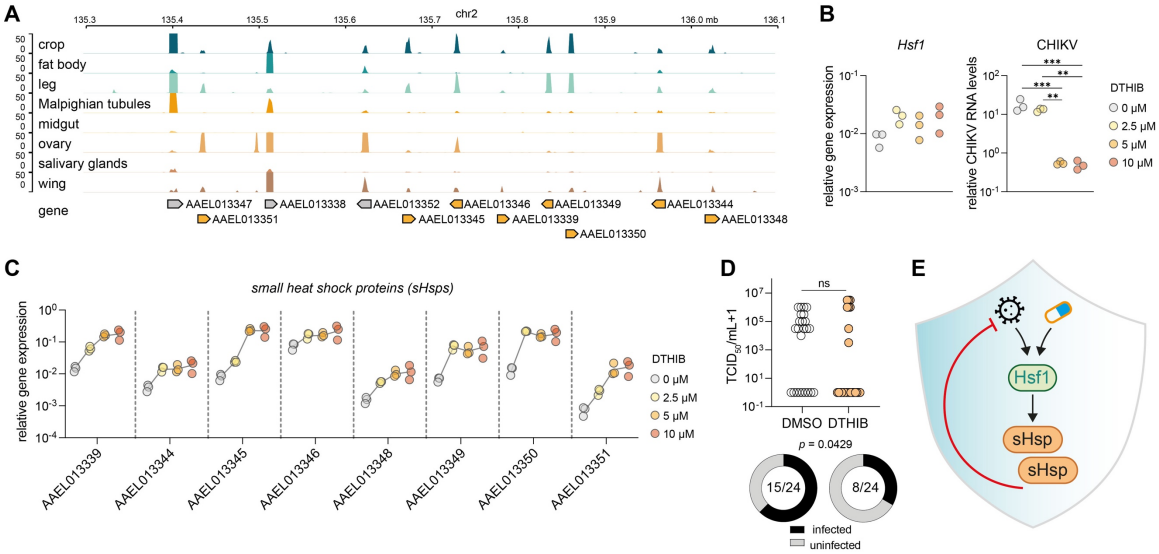

Figure 4. Antiviral activity of the Hsf1-sHsp axis *in vivo*.

(A) Genome browser tracks of RNA-seq showing the expression of *sHsp* genes in the indicated tissues.
(B) Relative *Hsf1* expression and CHIKV RNA copies by RT-qPCR in Aag2 cells upon DTHIB treatment at 12 hpi of CHIKV (MOI = 5) in biological triplicates, shown as dots. A series of DTHIB concentrations were tested and is shown in different colors. Symbols denote statistical significance in one-way ANOVA (** $p < 0.01$, *** $p < 0.001$).
(C) Relative *sHsp* expression to the house-keeping gene *LAP* by RT-qPCR in Aag2 cells upon DTHIB treatment at 12 hpi of CHIKV (MOI = 5) in biological triplicates, shown as dots. A series of DTHIB concentrations were tested and is shown in different colors. Trend lines of the mean of three independent experiments were plotted.
(D) Mosquito CHIKV infection status at 3 dpf with DTHIB treatment. 3–5-day-old *Ae. aegypti* female mosquitoes were fed with blood containing CHIKV and DTHIB (0.4 mM, orange) or DMSO as a control (white). For virus titer comparison, Mann-Whitney test was performed (ns, not significant). The infection rate of whole mosquitoes from each group was plotted as pie charts and compared using Chi-squared test, with the *p* value labeled.
(E) A working model for the antiviral activity of the Hsf1-sHsp cascade in mosquitoes.

449 **References**

450 1. Souza-Neto, J.A., J.R. Powell, and M. Bonizzoni, *Aedes aegypti vector competence studies:*
451 *A review.* Infection, Genetics and Evolution, 2019. **67**: p. 191-209.
452 2. Diagne, C., et al., *High and rising economic costs of biological invasions worldwide.* Nature,
453 2021: p. 1-6.
454 3. Weaver, S.C. and W.K. Reisen, *Present and future arboviral threats.* Antiviral research,
455 2010. **85**(2): p. 328-345.
456 4. Chibueze, E.C., et al., *Zika virus infection in pregnancy: a systematic review of disease*
457 *course and complications.* Reproductive health, 2017. **14**(1): p. 1-14.
458 5. Brady, O.J. and S.I. Hay, *The global expansion of dengue: how Aedes aegypti mosquitoes*
459 *enabled the first pandemic arbovirus.* Annual review of entomology, 2020. **65**: p. 191-208.
460 6. Paty, M., et al., *Large number of imported chikungunya cases in mainland France, 2014: a*
461 *challenge for surveillance and response.* Eurosurveillance, 2014. **19**(28): p. 20856.
462 7. Venturi, G., et al., *Detection of a chikungunya outbreak in Central Italy, August to*
463 *September 2017.* Eurosurveillance, 2017. **22**(39): p. 17-00646.
464 8. Burt, F.J., et al., *Chikungunya virus: an update on the biology and pathogenesis of this*
465 *emerging pathogen.* The Lancet Infectious Diseases, 2017. **17**(4): p. e107-e117.
466 9. Tomasello, D. and P. Schlagenhauf, *Chikungunya and dengue autochthonous cases in*
467 *Europe, 2007–2012.* Travel medicine and infectious disease, 2013. **11**(5): p. 274-284.
468 10. Calba, C., et al., *Preliminary report of an autochthonous chikungunya outbreak in France,*
469 *July to September 2017.* Eurosurveillance, 2017. **22**(39): p. 17-00647.
470 11. Rocklöv, J., et al., *Using big data to monitor the introduction and spread of chikungunya,*
471 *Europe, 2017.* Emerging infectious diseases, 2019. **25**(6): p. 1041.
472 12. Farjana, T. and N. Tuno, *Multiple blood feeding and host-seeking behavior in Aedes*
473 *aegypti and Aedes albopictus (Diptera: Culicidae).* Journal of medical entomology, 2013.
474 **50**(4): p. 838-846.
475 13. Manore, C.A., et al., *Defining the risk of Zika and chikungunya virus transmission in human*
476 *population centers of the eastern United States.* PLoS neglected tropical diseases, 2017.
477 **11**(1): p. e0005255.
478 14. Baldacchino, F., et al., *Control methods against invasive Aedes mosquitoes in Europe: a*
479 *review.* Pest management science, 2015. **71**(11): p. 1471-1485.
480 15. Merkling, S.H. and R.P. van Rij, *Beyond RNAi: antiviral defense strategies in Drosophila*
481 *and mosquito.* Journal of insect physiology, 2013. **59**(2): p. 159-170.
482 16. Mussabekova, A., L. Daeffler, and J.-L. Imler, *Innate and intrinsic antiviral immunity in*
483 *Drosophila.* Cellular and Molecular Life Sciences, 2017. **74**(11): p. 2039-2054.
484 17. Kingsolver, M.B., Z. Huang, and R.W. Hardy, *Insect antiviral innate immunity: pathways,*
485 *effectors, and connections.* Journal of molecular biology, 2013. **425**(24): p. 4921-4936.
486 18. Machado, S.R., T. van der Most, and P. Miesen, *Genetic determinants of antiviral*
487 *immunity in dipteran insects–Compiling the experimental evidence.* Developmental &
488 Comparative Immunology, 2021. **119**: p. 104010.
489 19. Van Rij, R.P., et al., *The RNA silencing endonuclease Argonaute 2 mediates specific*
490 *antiviral immunity in Drosophila melanogaster.* Genes & development, 2006. **20**(21): p.
491 2985-2995.

492 20. Wang, X.-H., et al., *RNA interference directs innate immunity against viruses in adult*
493 *Drosophila.* Science, 2006. **312**(5772): p. 452-454.
494 21. Galiana-Arnoux, D., et al., *Essential function in vivo for Dicer-2 in host defense against RNA*
495 *viruses in drosophila.* Nature immunology, 2006. **7**(6): p. 590-597.
496 22. Tafesh-Edwards, G. and I. Eleftherianos, *Drosophila immunity against natural and*
497 *nonnatural viral pathogens.* Virology, 2020. **540**: p. 165-171.
498 23. Vega-Rúa, A., et al., *High level of vector competence of Aedes aegypti and Aedes*
499 *albopictus from ten American countries as a crucial factor in the spread of Chikungunya*
500 *virus.* Journal of virology, 2014. **88**(11): p. 6294-6306.
501 24. Coffey, L.L., A.-B. Failloux, and S.C. Weaver, *Chikungunya virus–vector interactions.*
502 Viruses, 2014. **6**(11): p. 4628-4663.
503 25. McFarlane, M., et al., *Characterization of Aedes aegypti innate-immune pathways that*
504 *limit Chikungunya virus replication.* PLoS Negl Trop Dis, 2014. **8**(7): p. e2994.
505 26. Buchman, A., et al., *Engineered resistance to Zika virus in transgenic Aedes aegypti*
506 *expressing a polycistronic cluster of synthetic small RNAs.* Proceedings of the National
507 Academy of Sciences, 2019. **116**(9): p. 3656-3661.
508 27. Magalhaes, T., et al., *Induction of RNA interference to block Zika virus replication and*
509 *transmission in the mosquito Aedes aegypti.* Insect biochemistry and molecular biology,
510 2019. **111**: p. 103169.
511 28. Franz, A.W., et al., *Engineering RNA interference-based resistance to dengue virus type 2*
512 *in genetically modified Aedes aegypti.* Proceedings of the National Academy of Sciences,
513 2006. **103**(11): p. 4198-4203.
514 29. Sánchez-Vargas, I., et al., *Dengue virus type 2 infections of Aedes aegypti are modulated*
515 *by the mosquito's RNA interference pathway.* PLoS Pathog, 2009. **5**(2): p. e1000299.
516 30. Khoo, C.C., et al., *The RNA interference pathway affects midgut infection-and escape*
517 *barriers for Sindbis virus in Aedes aegypti.* BMC microbiology, 2010. **10**(1): p. 1-12.
518 31. Angleró-Rodríguez, Y.I., et al., *Aedes aegypti molecular responses to Zika virus:*
519 *modulation of infection by the toll and jak/stat immune pathways and virus host factors.*
520 Frontiers in microbiology, 2017. **8**: p. 2050.
521 32. Xi, Z., J.L. Ramirez, and G. Dimopoulos, *The Aedes aegypti toll pathway controls dengue*
522 *virus infection.* PLoS Pathog, 2008. **4**(7): p. e1000098.
523 33. Behura, S.K., et al., *Global cross-talk of genes of the mosquito Aedes aegypti in response*
524 *to dengue virus infection.* PLoS Negl Trop Dis, 2011. **5**(11): p. e1385.
525 34. Barletta, A.B.F., et al., *Microbiota activates IMD pathway and limits Sindbis infection in*
526 *Aedes aegypti.* Parasites & vectors, 2017. **10**(1): p. 1-9.
527 35. Souza-Neto, J.A., S. Sim, and G. Dimopoulos, *An evolutionary conserved function of the*
528 *JAK-STAT pathway in anti-dengue defense.* Proceedings of the National Academy of
529 Sciences, 2009. **106**(42): p. 17841-17846.
530 36. Scholte, F.E., et al., *Characterization of synthetic Chikungunya viruses based on the*
531 *consensus sequence of recent E1-226V isolates.* PloS one, 2013. **8**(8): p. e71047.
532 37. Machado, S.R., et al., *The DEAD-box RNA helicase Dhx15 controls glycolysis and arbovirus*
533 *replication in Aedes aegypti mosquito cells.* bioRxiv, 2022: p.
534 2022.06.22.497281.
535 38. Garrido, C., et al., *The small heat shock proteins family: the long forgotten chaperones.*
536 The international journal of biochemistry & cell biology, 2012. **44**(10): p. 1588-1592.

537 39. Taguwa, S., et al., *Defining Hsp70 subnetworks in dengue virus replication reveals key*
538 *vulnerability in flavivirus infection.* Cell, 2015. **163**(5): p. 1108-1123.
539 40. Taguwa, S., et al., *Zika virus dependence on host Hsp70 provides a protective strategy*
540 *against infection and disease.* Cell reports, 2019. **26**(4): p. 906-920. e3.
541 41. Wimalasiri-Yapa, B.R., et al., *Temperature modulates immune gene expression in*
542 *mosquitoes during arbovirus infection.* Open biology, 2021. **11**(1): p. 200246.
543 42. Dudchenko, O., et al., *De novo assembly of the Aedes aegypti genome using Hi-C yields*
544 *chromosome-length scaffolds.* Science, 2017. **356**(6333): p. 92-95.
545 43. Nora, E.P., et al., *Spatial partitioning of the regulatory landscape of the X-inactivation*
546 *centre.* Nature, 2012. **485**(7398): p. 381-385.
547 44. Schoenfelder, S., et al., *The pluripotent regulatory circuitry connecting promoters to their*
548 *long-range interacting elements.* Genome research, 2015. **25**(4): p. 582-597.
549 45. Qu, J., et al., *Chromatin profiling identifies transcriptional readthrough as a conserved*
550 *mechanism for piRNA cluster biogenesis in mosquitoes.* bioRxiv, 2022.
551 46. Stasevich, T.J., et al., *Regulation of RNA polymerase II activation by histone acetylation in*
552 *single living cells.* Nature, 2014. **516**(7530): p. 272-275.
553 47. Hampsey, M. and D. Reinberg, *Tails of intrigue: phosphorylation of RNA polymerase II*
554 *mediates histone methylation.* Cell, 2003. **113**(4): p. 429-432.
555 48. Yoon, Y.J., et al., *KRIBB11 inhibits HSP70 synthesis through inhibition of heat shock factor*
556 *1 function by impairing the recruitment of positive transcription elongation factor b to the*
557 *hsp70 promoter.* Journal of Biological Chemistry, 2011. **286**(3): p. 1737-1747.
558 49. Neef, D.W., M.L. Turski, and D.J. Thiele, *Modulation of heat shock transcription factor 1*
559 *as a therapeutic target for small molecule intervention in neurodegenerative disease.* PLoS
560 biology, 2010. **8**(1): p. e1000291.
561 50. Hubálek, Z., *Mosquito-borne viruses in Europe.* Parasitology research, 2008. **103**: p. 29-43.
562 51. Vanlandingham, D.L., et al., *Differential infectivities of o'nyong-nyong and chikungunya*
563 *virus isolates in Anopheles gambiae and Aedes aegypti mosquitoes.* The American journal
564 of tropical medicine and hygiene, 2005. **72**(5): p. 616-621.
565 52. Dong, B., et al., *Targeting therapy-resistant prostate cancer via a direct inhibitor of the*
566 *human heat shock transcription factor 1.* Science Translational Medicine, 2020. **12**(574):
567 p. eabb5647.
568 53. Sanders, H.R., et al., *Sindbis virus induces transport processes and alters expression of*
569 *innate immunity pathway genes in the midgut of the disease vector, Aedes aegypti.* Insect
570 biochemistry and molecular biology, 2005. **35**(11): p. 1293-1307.
571 54. Liu, W.-Q., et al., *The Ras/ERK signaling pathway couples antimicrobial peptides to*
572 *mediate resistance to dengue virus in Aedes mosquitoes.* PLoS neglected tropical diseases,
573 2020. **14**(8): p. e0008660.
574 55. Chen, T.-Y., et al., *Profiling transcriptional response of dengue-2 virus infection in midgut*
575 *tissue of Aedes aegypti.* Frontiers in Tropical Diseases, 2021. **2**: p. 708817.
576 56. Howe, M.K., et al., *An inducible heat shock protein 70 small molecule inhibitor*
577 *demonstrates anti-dengue virus activity, validating Hsp70 as a host antiviral target.*
578 Antiviral research, 2016. **130**: p. 81-92.
579 57. Ferreira, P.G., et al., *Temperature dramatically shapes mosquito gene expression with*
580 *consequences for mosquito–Zika virus interactions.* Frontiers in microbiology, 2020. **11**: p.
581 901.

582 58. Haslbeck, M., et al., *Some like it hot: the structure and function of small heat-shock*
583 *proteins.* Nature structural & molecular biology, 2005. **12**(10): p. 842-846.
584 59. Basha, E., et al., *The identity of proteins associated with a small heat shock protein during*
585 *heat stress in vivo indicates that these chaperones protect a wide range of cellular*
586 *functions.* Journal of Biological Chemistry, 2004. **279**(9): p. 7566-7575.
587 60. Vecchi, G., et al., *Proteome-wide observation of the phenomenon of life on the edge of*
588 *solubility.* Proceedings of the National Academy of Sciences, 2020. **117**(2): p. 1015-1020.
589 61. Haslbeck, M., S. Weinkauf, and J. Buchner, *Small heat shock proteins: simplicity meets*
590 *complexity.* Journal of Biological Chemistry, 2019. **294**(6): p. 2121-2132.
591 62. Dabbaghizadeh, A. and R.M. Tanguay, *Structural and functional properties of proteins*
592 *interacting with small heat shock proteins.* Cell Stress and Chaperones, 2020. **25**(4): p.
593 629-637.
594 63. Hahn, C.S., et al., *Infectious Sindbis virus transient expression vectors for studying antigen*
595 *processing and presentation.* Proceedings of the National Academy of Sciences, 1992.
596 **89**(7): p. 2679-2683.
597 64. Hermanns, K., et al., *Agua Salud alphavirus defines a novel lineage of insect-specific*
598 *alphaviruses discovered in the New World.* The Journal of general virology, 2020. **101**(1):
599 p. 96.
600 65. Varghese, F.S., et al., *The antiviral alkaloid berberine reduces chikungunya virus-induced*
601 *mitogen-activated protein kinase signaling.* Journal of virology, 2016. **90**(21): p. 9743-
602 9757.
603 66. Reed, L.J. and H. Muench, *A simple method of estimating fifty per cent endpoints.*
604 American journal of epidemiology, 1938. **27**(3): p. 493-497.
605 67. Coleman, J., J. Juhn, and A.A. James, *Dissection of midgut and salivary glands from Ae.*
606 *aegypti mosquitoes.* JoVE (Journal of Visualized Experiments), 2007(5): p. e228.
607 68. Livak, K.J. and T.D. Schmittgen, *Analysis of relative gene expression data using real-time*
608 *quantitative PCR and the 2− ΔΔCT method.* methods, 2001. **25**(4): p. 402-408.
609 69. Andrews, S., *FastQC: a quality control tool for high throughput sequence data*. 2010,
610 Babraham Bioinformatics, Babraham Institute, Cambridge, United Kingdom.
611 70. Dobin, A., et al., *STAR: ultrafast universal RNA-seq aligner.* Bioinformatics, 2013. **29**(1): p.
612 15-21.
613 71. Trapnell, C., et al., *Differential analysis of gene regulation at transcript resolution with*
614 *RNA-seq.* Nature biotechnology, 2013. **31**(1): p. 46-53.
615 72. Love, M.I., W. Huber, and S. Anders, *Moderated estimation of fold change and dispersion*
616 *for RNA-seq data with DESeq2.* Genome Biology, 2014. **15**(12): p. 550.
617 73. Kolde, R., *Pheatmap: pretty heatmaps.* R package version, 2012. **1**(2): p. 726.
618 74. Szklarczyk, D., et al., *The STRING database in 2021: customizable protein–protein*
619 *networks, and functional characterization of user-uploaded gene/measurement sets.*
620 Nucleic acids research, 2021. **49**(D1): p. D605-D612.
621 75. Paysan-Lafosse, T., et al., *InterPro in 2022.* Nucleic Acids Research, 2023. **51**(D1): p. D418-
622 D427.
623 76. Ramírez, F., et al., *High-resolution TADs reveal DNA sequences underlying genome*
624 *organization in flies.* Nature communications, 2018. **9**(1): p. 1-15.
625 77. Ramírez, F., et al., *deepTools: a flexible platform for exploring deep-sequencing data.*
626 Nucleic acids research, 2014. **42**(W1): p. W187-W191.

627 78. Zhang, Y., et al., *Model-based analysis of ChIP-Seq (MACS).* Genome biology, 2008. **9**(9):
628 p. 1-9.
629 79. Heinz, S., et al., *Simple combinations of lineage-determining transcription factors prime*
630 *cis-regulatory elements required for macrophage and B cell identities.* Molecular cell,
631 2010. **38**(4): p. 576-589.

632

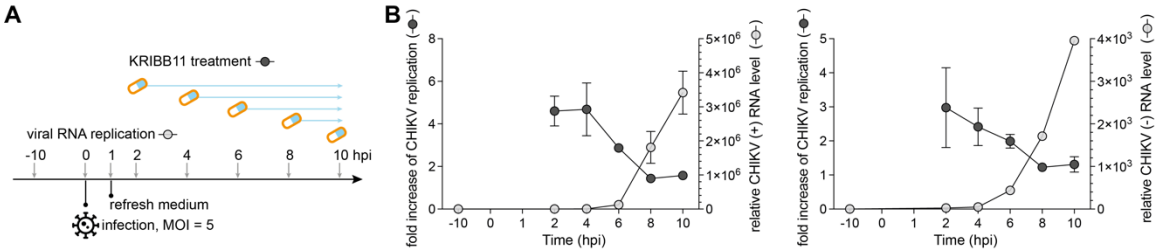

Figure S1. The time-of-addition assay of KRIBB11, related to Figure 3

(A) Schematic illustration of the time-of-addition assay, with KRIBB11 added at different time points during CHIKV infection (MOI=5). Cell culture medium was refreshed to wash away unbound virus particles at 1 hpi. Cells treated with either KRIBB11 (dark gray) or DMSO (gray) were harvested at each indicated time point.

(B) The effect of KRIBB11 (10 μM) on virus replication was determined with RT-qPCR on both positive sense RNA (+, left) and negative sense RNA (-, right). Data are presented as means ± SD of three independent experiments, with DMSO serving as control.

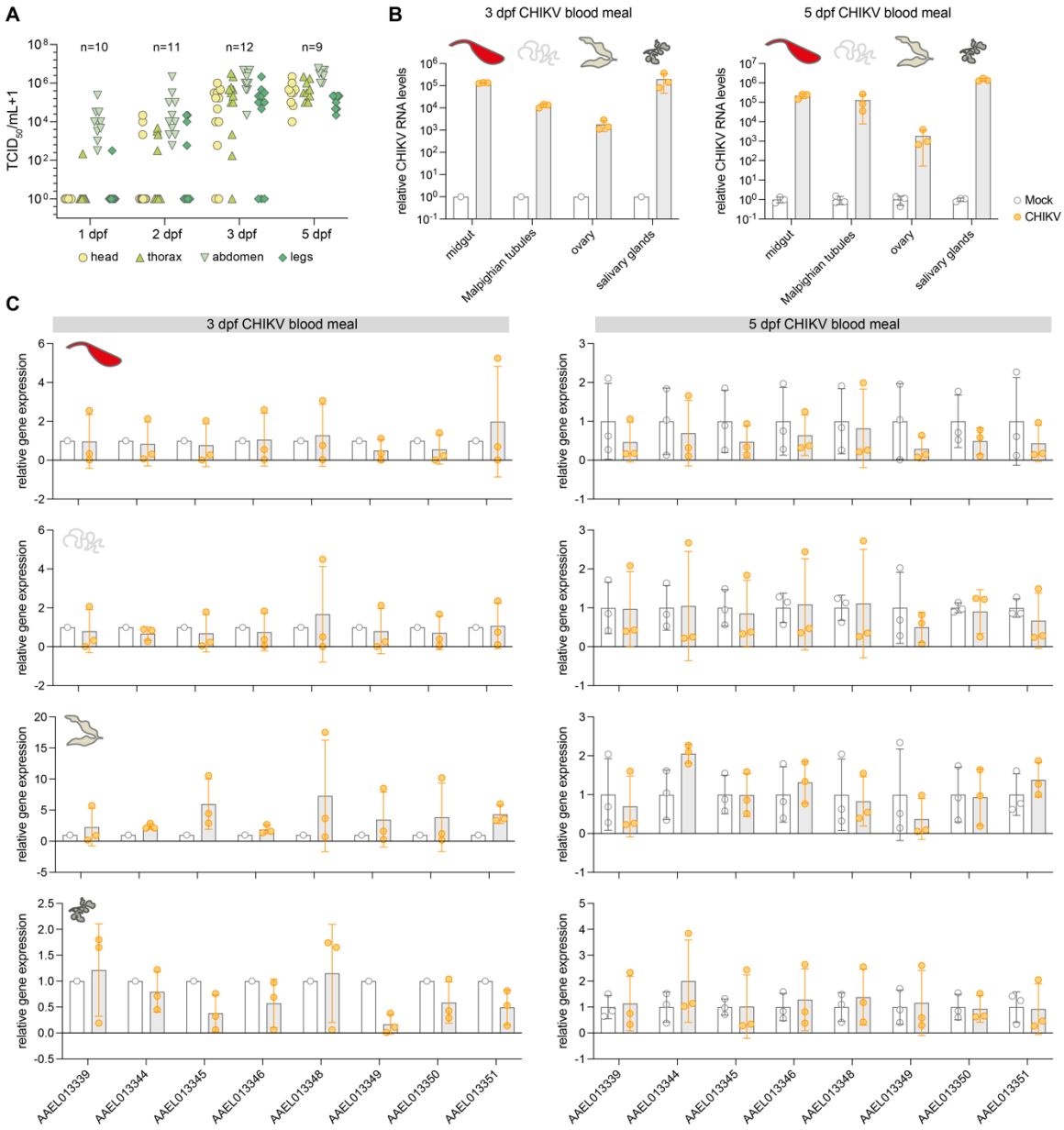

Figure S2. Inspection of *sHsp* gene expression in different tissues, related to Figure 4

(A) In vivo CHIKV replication kinetics. 3–5-day-old female *Ae. aegypti* mosquitoes were fed with CHIKV infectious blood. At the indicated time points, head, thorax, abdomen, and legs from individual mosquitoes were dissected and used for titration. Number of mosquitoes per time point are indicated on top.

(B-C) CHIKV levels in midguts, Malpighian tubules, ovaries and salivary glands at 3 d and 5 d after infectious blood meal. RT-qPCR was performed to quantify CHIKV RNA copies (B) and expression of sHsp genes (C). Dissected organs from 15 mosquitoes were pooled as one sample and shown as one dot. Data are presented as mean values ± SD of three biological replicates. Mock infections are shown as white symbols and bars, CHIKV infections as orange symbols and grey bars.

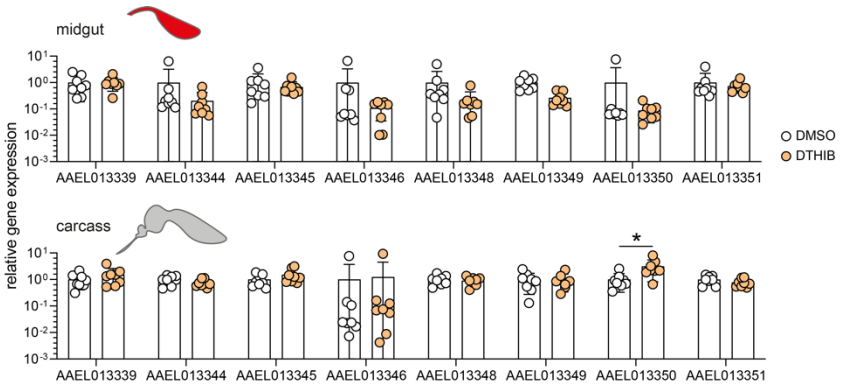

Figure S3. *sHsp* gene expression in different tissues after DTHIB treatment, related to Figure 4

3–5-day-old female *Ae. aegypti* mosquitoes were fed with blood containing either DMSO (control, white) or DTHIB (treatment, orange). At 3 dpi, midgut and carcass from 40 mosquitoes (5 mosquitoes per group, plotted as one data point) were dissected and used for qPCR analysis of *sHsp* gene expression. Bars represent means ± SD; * $p < 0.05$, unpaired t-test.

661 **Table S1. Differentially expressed genes (DEgenes) upon CHIKV infection at different time points.**

time point	gene regulation upon CHIKV infection	DEgenes	log2FoldChange	padj
4 hpi CHIKV	downregulated genes	*AAEL000080*	1.82	1.10E-02
8 hpi CHIKV	upregulated genes	*AAEL022059*	-5.40	7.94E-06
		AAEL007830	-1.02	5.37E-03
		AAEL027610	-5.73	3.01E-25
		AAEL022253	-5.62	2.94E-23
		AAEL017975	-4.94	3.29E-23
		AAEL017976	-5.06	3.45E-22
		AAEL020330	-6.31	1.16E-10
		AAEL006883	-1.07	3.80E-02
		AAEL013351	-3.53	3.29E-15
		AAEL013345	-2.60	7.25E-12
		AAEL013346	-1.53	8.79E-04
		AAEL013339	-2.34	1.09E-10
		AAEL013349	-2.82	7.54E-13
		AAEL013350	-2.74	5.09E-13
		AAEL013344	-2.27	1.55E-10
		AAEL013348	-2.13	1.55E-10
		AAEL001800	-1.30	3.07E-06
		AAEL000566	-2.08	1.25E-03
		AAEL015631	-1.69	6.73E-09
	downregulated genes	*AAEL000080*	1.42	2.21E-06
		AAEL000006	1.78	1.00E-02
48 hpi CHIKV	upregulated genes	*AAEL005641*	-2.38	2.94E-02
		AAEL006685	-1.70	1.34E-04
		AAEL010557	-1.50	1.20E-02
		AAEL004979	-1.35	3.16E-02
		AAEL011957	-1.25	2.94E-02
		AAEL010924	-1.23	6.44E-03
		AAEL010253	-1.10	7.40E-03
	downregulated genes	*AAEL003950*	-1.05	3.50E-02
		AAEL007298	1.01	3.90E-02
		AAEL007920	1.01	7.31E-03
		AAEL023822	1.02	1.29E-02
		AAEL005739	1.02	3.10E-02
		AAEL003524	1.04	1.95E-03
		AAEL007129	1.07	3.02E-02
		AAEL010411	1.08	3.10E-02
		AAEL002102	1.10	3.81E-02
		AAEL002531	1.11	4.01E-04
		AAEL002861	1.15	1.98E-02
		AAEL007109	1.15	3.81E-04
		AAEL024100	1.15	4.21E-02
		AAEL010529	1.16	7.40E-03
		AAEL013065	1.17	1.44E-02
		AAEL007476	1.18	7.53E-04
		AAEL000663	1.21	1.27E-04
		AAEL011703	1.21	1.63E-03
		AAEL018301	1.21	7.38E-04
		AAEL005766	1.22	1.00E-03
		AAEL026751	1.23	2.28E-04

	AAEL019957	1.24	1.29E-02
	AAEL001315	1.25	1.29E-02
	AAEL012125	1.26	5.37E-03
	AAEL005213	1.27	2.13E-03
	AAEL006904	1.28	4.21E-02
	AAEL006815	1.28	7.17E-03
	AAEL000248	1.31	3.89E-03
	AAEL011371	1.31	5.12E-03
	AAEL008664	1.31	1.34E-04
	AAEL003965	1.33	3.89E-03
	AAEL009339	1.33	2.54E-02
	AAEL009387	1.33	1.27E-04
	AAEL007342	1.34	7.85E-03
	AAEL017458	1.38	7.31E-03
	AAEL007830	1.38	7.94E-04
	AAEL006449	1.39	1.63E-03
	AAEL019499	1.48	7.58E-04
	AAEL009126	1.49	8.93E-03
	AAEL024007	1.50	8.66E-03
	AAEL006180	1.55	3.16E-02
	AAEL006895	1.61	2.23E-04
	AAEL000834	1.65	1.60E-07
	AAEL012014	1.74	8.83E-05
	AAEL005850	1.85	1.26E-02
	AAEL013350	1.95	1.27E-04
	AAEL002796	1.99	1.74E-03
	AAEL020524	2.05	7.95E-04
	AAEL001548	2.09	6.20E-04
	AAEL021456	2.22	1.34E-04
	AAEL013349	2.31	8.83E-05
	AAEL012522	3.11	1.01E-12

664 **Table S2. oligonucleotide information.**

species	Oligo Name	sequence
Ae. aegypti	AAEL019713 (Hsf1)_T7-1F	TAATACGACTCACTATAGGGAGATCAATCAGATGGGTTCCACA
Ae. aegypti	AAEL019713 (Hsf1)_T7-1R	TAATACGACTCACTATAGGGAGATCCACAAGGCTTCATTTTCC
Ae. aegypti	AAEL013339 (sHsps)_T7-1F	TAATACGACTCACTATAGGGAGATTGGACGACGAACTTCAGGA
Ae. aegypti	AAEL013339 (sHsps)_T7-1R	TAATACGACTCACTATAGGGAGATGGAATGGGTCGCTCTTTCT
Ae. aegypti	AAEL013344 (sHsps)_T7-1F	TAATACGACTCACTATAGGGAGATGGGATGACTGCTGGGATAC
Ae. aegypti	AAEL013344 (sHsps)_T7-1R	TAATACGACTCACTATAGGGAGATGGTTGCAATCATGTCCAGC
Ae. aegypti	AAEL017975 (Hsp70)_T7-1F	TAATACGACTCACTATAGGGAGATGTTCAACGATGCTGGCAAA
Ae. aegypti	AAEL017975 (Hsp70)_T7-1R	TAATACGACTCACTATAGGGAGAATCCGAGCACAGTTCCTCAA
Ae. aegypti	AAEL017975 (Hsp70)_T7-2F	TAATACGACTCACTATAGGGAGAAATGGACAAGCGCTCAATCC
Ae. aegypti	AAEL017975 (Hsp70)_T7-2R	TAATACGACTCACTATAGGGAGAGGTACTTTTCTGCGTCGGAC
Ae. aegypti	LAP_AAEL006169_qPCR_F	GTGCTCATTCACCAACATCG
Ae. aegypti	LAP_AAEL006169_qPCR_R	AACTTGGCCGCAACAAATAC
Ae. aegypti	AAEL019713_qPCR_F	AGCTCTGGAGACTGGTGGAA
Ae. aegypti	AAEL019713_qPCR_R	TGATGAAGCTTCTCCCATCC
Ae. aegypti	AAEL013339_qPCR_F	GCTCTTGTGCCTGTTTTGCT
Ae. aegypti	AAEL013339_qPCR_R	CGGGGTAGGTCATCATCCAA
Ae. aegypti	AAEL013345_qPCR_F	GCTCGACTTCTGAACAAACGA
Ae. aegypti	AAEL013345_qPCR_R	TATCTTCCGGGTAGAGGCCA
Ae. aegypti	AAEL013350_qPCR_F	GTGATTTGTGGGATGGCTGC
Ae. aegypti	AAEL013350_qPCR_R	GTTGTCTGTCGAGGTGTTGG
Ae. aegypti	AAEL013344_qPCR_F	GAAGGACCCAAAGCGATTCC
Ae. aegypti	AAEL013344_qPCR_R	AATCCTGCAGTTGTTTCGCT
Ae. aegypti	AAEL013346_qPCR_F	ATCGGATGGCATTTTGACGG
Ae. aegypti	AAEL013346_qPCR_R	GGAATCGCCTTTGGTCCTTC
Ae. aegypti	AAEL013348_qPCR_F	ACGGTCACTGCTCTGAAGAA
Ae. aegypti	AAEL013348_qPCR_R	CCATCTTTTCACCGCCTTCC
Ae. aegypti	AAEL013349_qPCR_F	GCAACCGGTGAAAAGACTGA
Ae. aegypti	AAEL013349_qPCR_R	TGCATTACCGTTCACTTGTCC
Ae. aegypti	AAEL013351_qPCR_F	ACAAAAGGAAAGGATCGCGG
Ae. aegypti	AAEL013351_qPCR_R	GGCTTATCCGCTTCAGGTTT
Ae. aegypti	AAEL017975_qPCR_F	CCAGTTGAAGCAATCCCTCG
Ae. aegypti	AAEL017975_qPCR_R	GCATTTGTCCTTCACGGTGT
Ae. albopictus	RpL5_AALF020547_qPCR_F	TCGCTTACGCCCGCATTGAGGGTGAT
Ae. albopictus	RpL5_AALF020547_qPCR_R	TCGCCGGTCACATCGGTACAGCCA
An. gambiae	RpL5_AGAP009031_qPCR_F	TCGGCCTGCACGTCGCCAACTACA
An. gambiae	RpL5_AGAP009031_qPCR_R	GGGATCCTGATGGAGGCGTGGGCG
virus	CHIKV_positive_F	TCTCCGTACGTGAAGTGCTG
virus	CHIKV_positive_R	ACATGTGCTTCGCTCAACTG
virus	CHIKV_Tag_ns3_RT	CCTCCGCGGCCGTCATGGTGGCGAGCGCGTAAGTCCAAGGGAAT
virus	CHIKV_negative_F	CCTCCGCGGCCGTCATGGTGGCGA
virus	CHIKV_negative_R	AGCATCCAGGTCTGACGGG
virus	SINV_F	AACTCTGCCACAGATCAGCC
virus	SINV_R	GGGGCAGAAGGTTGCAGTAT
virus	ASALV_F	CTCGAAGAGAGGCTCACCAC
virus	ASALV_R	CGCAGAAGTAAGGCGGTTTG
virus	DENV_F	TATGACAGGAGACATCAAAGGA
virus	DENV_R	CCGCTGACATGAGTTTTGAGTC
virus	ONNV_F	CGCAGCTTACGGGTTTCATA
virus	ONNV_R	GCAACGCCTTCAGAAACGC

665